Covalent Grafting of Redox-Active Molecules to Vertically Aligned Carbon Nanofiber Arrays via "Click" Chemistry

Elizabeth C. Landis and Robert J. Hamers*

Department of Chemistry, University of Wisconsin Madison, 1101 University Avenue, Madison, Wisconsin 53706

Received October 22, 2008. Revised Manuscript Received December 20, 2008

Electrochemically active ferrocene groups were covalently linked to vertically aligned carbon nanofibers (VACNFs) in a simple and efficient manner via the Cu(I)-catalyzed azide alkyne cycloaddition (CuAAC), one form of "click" chemistry. The VACNFs were terminated with azide groups followed by the attachment of ethynylferrocene through a 1,4-disubstituted 1,2,3-triazole linkage. Our results show that the CuAAC reaction goes to completion in one hour and provides highly stable attachment of electrochemically active ferrocene groups to the nanofibers. X-ray photoelectron spectroscopy measurements of the density of surface-bound ferrocene molecules are in good agreement with those determined by cyclic voltammetry. The rates of electron transfer were found to be slightly faster than those measured previously through alkyl linkages to the VACNF surface. Stability tests show that the covalently grafted ferrocene groups are stable for more than 1500 repeated cyclic voltammograms and over a potential window of >1.5 V, limited by the solvent. These results suggest that the use of "click" chemistry with VACNFs provides a facile route toward synthesis of high-surface-area electrodes with high stability and tailored electrochemical properties.

Introduction

Recent advances in the synthesis and characterization of nanotubes, nanofibers, and related nanoscale carbons have shown these materials to have many outstanding properties, including high electrical conductivity and chemical stability.[1−9] Although the chemical stability of carbon is often highly desirable, there is great interest in selectively enhancing and controlling the properties of carbon-based materials by covalently linking more complex molecules to the surface, yielding "smart carbons" that have specific types of chemical or electrochemical reactions for applications in sensing, electroanalysis, energy storage, and catalysis.[4,5,7,10−12]

The copper-catalyzed azide−alkyne cycloaddition (CuAAC) has come into wide use since its introduction in 2002.[13,14] The reaction couples a terminal azide with an alkyne, creating a 1,4-disubstituted 1,2,3-triazole linkage via a [3 + 2] Huisgen cycloaddition. This reaction is considered an excellent example of "click" chemistry because of its selectivity and tolerance to a variety of reaction conditions.[15] Recently, the CuAAC reaction has been used to chemically modify a number of different surfaces[16] including gold,[17] silicon,[18,19] and graphitic surfaces of pyrolized photoresist.[20] The attachment is particularly promising because it has been shown that the reaction on gold is quantitative under mild reaction conditions and because the 1,2,3-triazole linkage provides excellent stability.[17] Previous work on gold electrodes has also shown that conjugation in the tethering chain can promote stronger electronic coupling between the redox active group and the surface, leading to faster electron transfer rates.[16,21−23]

* Corresponding author. E-mail: rjhamers@wisc.edu.

(1) McKnight, T. E.; Peeraphatdit, C.; Jones, S. W.; Fowlkes, J. D.; Fletcher, B. L.; Klein, K. L.; Melechko, A. V.; Doktycz, M. J.; Simpson, M. L. *Chem. Mater.* **2006**, *18*, 3203.
(2) Melechko, A. V.; Klein, K. L.; Fowlkes, J. D.; Hensley, D. K.; Merkulov, I. A.; McKnight, T. E.; Rack, P. D.; Horton, J. A.; Simpson, M. L. *J. Appl. Phys.* **2007**, 102.
(3) Melechko, A. V.; Merkulov, V. I.; McKnight, T. E.; Guillorn, M. A.; Klein, K. L.; Lowndes, D. H.; Simpson, M. L. *J. Appl. Phys.* **2005**, 97.
(4) Baker, S. E.; Colavita, P. E.; Tse, K. Y.; Hamers, R. J. *Chem. Mater.* **2006**, *18*, 4415.
(5) Baker, S. E.; Tse, K. Y.; Hindin, E.; Nichols, B. M.; Clare, T. L.; Hamers, R. J. *Chem. Mater.* **2005**, *17*, 4971.
(6) Baughman, R. H.; Zakhidov, A. A.; de Heer, W. A. *Science* **2002**, *297*, 787.
(7) Kim, C.; Kim, Y. J.; Kim, Y. A.; Yanagisawa, T.; Park, K. C.; Endo, M.; Dresselhaus, M. S. *J. Appl. Phys.* **2004**, *96*, 5903.
(8) Musameh, M.; Lawrence, N. S.; Wang, J. *Electrochem. Commun.* **2005**, *7*, 14.
(9) Banks, C. E.; Ji, X. B.; Crossley, A.; Compton, R. G. *Electroanalysis* **2006**, *18*, 2137.
(10) Yang, W. S.; Auciello, O.; Butler, J. E.; Cai, W.; Carlisle, J. A.; Gerbi, J.; Gruen, D. M.; Knickerbocker, T.; Lasseter, T. L.; Russell, J. N.; Smith, L. M.; Hamers, R. J. *Nat. Mater.* **2002**, *1*, 253.
(11) Frackowiak, E.; Beguin, F. *Carbon* **2001**, *39*, 937.
(12) Baker, S. E.; Tse, K. Y.; Lee, C. S.; Hamers, R. J. *Diamond Relat. Mater.* **2006**, *15*, 433.
(13) Rostovtsev, V. V.; Green, L. G.; Fokin, V. V.; Sharpless, K. B. *Angew. Chem., Int. Ed.* **2002**, *41*, 2596.
(14) Tornoe, C. W.; Christensen, C.; Meldal, M. *J. Org. Chem.* **2002**, *67*, 3057.
(15) Kolb, H. C.; Finn, M. G.; Sharpless, K. B. *Angew. Chem., Int. Ed.* **2001**, *40*, 2004.
(16) Devaraj, N. K.; Collman, J. P. *QSAR Comb. Sci.* **2007**, *26*, 1253.
(17) Collman, J. P.; Devaraj, N. K.; Chidsey, C. E. D. *Langmuir* **2004**, *20*, 1051.
(18) Ciampi, S.; Bocking, T.; Kilian, K. A.; James, M.; Harper, J. B.; Gooding, J. J. *Langmuir* **2007**, *23*, 9320.
(19) Rohde, R. D.; Agnew, H. D.; Yeo, W. S.; Bailey, R. C.; Heath, J. R. *J. Am. Chem. Soc.* **2006**, *128*, 9518.
(20) Devadoss, A.; Chidsey, C. E. D. *J. Am. Chem. Soc.* **2007**, *129*, 5370.
(21) Creager, S.; Y.C., J.; Bamdad, C.; O'Connor, S.; MacLean, T.; Lam, E.; Chong, Y.; Olsen, G. T.; Luo, J.; Gozin, M.; Kayyem., J. F. *J. Am. Chem. Soc.* **1999**, *121*, 1059.
(22) Collman, J. P.; Devaraj, N. K.; Decreau, R. A.; Yang, Y.; Yan, Y. L.; Ebina, W.; Eberspacher, T. A.; Chidsey, C. E. D. *Science* **2007**, *315*, 1565.

10.1021/cm802869b CCC: $40.75
Published on Web 01/22/2009

Of the many forms of nanoscale carbon, vertically aligned carbon nanofibers (VACNFs) are particularly interesting because they have a unique molecular structure[3,24,25] that makes them especially attractive substrates for electrochemical and electrocatalytic reactions. VACNFs consist of graphene sheets arranged into stacked-cup and "bamboo" structures that expose large amounts of edge-plane graphite along the nanofibers sidewalls;[3] in comparison, carbon nanotubes expose only basal-plane graphite along their sidewalls. Because electron transfer rates on edge-plane graphite are $\sim 1 \times 10^5$ times higher than basal plane graphite,[26] this suggests that VACNFs are promising as scaffolds for electrocatalytic reactions. Furthermore, each nanofiber has a direct electrical connection to the underlying substrate.

Previous studies have grafted molecular layers to VACNFs using the photochemical grafting of alkenes[4,5] or via reaction with diazonium compounds.[4,5,12] The photochemical method uses ultraviolet light to link terminal alkenes to the surface, but is limited to alkenes that are stable under ultraviolet light and may not be effective on thick nanofiber arrays because of the strong optical absorption of the nanofibers. The diazonium method frequently forms multilayers due to the radical intermediates involved.[27,28] Although several other techniques[29] including oxidative methods[30,31] and acylation in concentrated nitric acid[32,33] have been used to functionalize VACNF surfaces, these methods require harsh reaction conditions and are difficult to control.

In this paper, we present a gentle method for covalently functionalizing VACNFs through a CuAAC reaction in which an azide group is bound to the surface and then linked with an alkyne. We demonstrate that this procedure leads to covalently grafted ferrocene groups exhibiting excellent electron-transfer rates and with extremely good stability in repeated cyclic voltammetry cycles.

Materials and Methods

Vertically aligned carbon nanofibers were grown in a custom-built plasma enhanced chemical vapor deposition system.[3,5,12,24,25] The nanofibers were grown on silicon substrates coated with 20 nm Mo, 20 nm Ti, and finally, 10 nm of Ni. The nanofibers were grown at a pressure of 4 torr in a flow of 100 standard cubic centimeters per minute (sccm) ammonia and 36 sccm acetylene, in a DC plasma at a power of 360 W. The nanofiber length is determined by the growth time. The nanofibers reported here were typically grown for 18 min, which yields fibers 1.0 ± 0.3 μm long. Nanofibers used for infrared spectroscopy experiments were grown for a shorter time of 5 min in order to retain sufficient reflectivity.

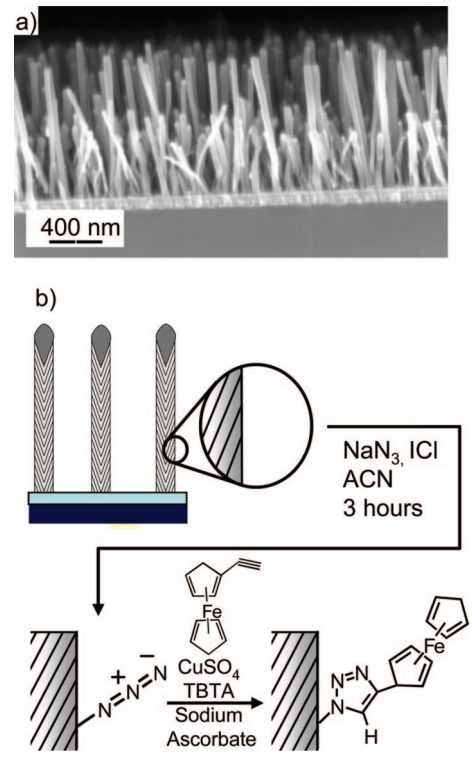

Figure 1. (a) SEM image of vertically aligned carbon nanofiber cross-section. (b) Reaction scheme of ferrocene attachment to the VACNF surface.

Results

Substrate Functionalization. Figure 1a shows a scanning electron microscope (SEM) image of the as-grown VACNFs. Ethynylferrocene was attached to the VACNFs following the procedure outlined in Figure 1b. The method for attaching an alkyne group to the surface follows the procedure of Devadoss, et al.[20] and consists of first linking an azide to the VACNF surface, followed by reaction of the azide with an acetylide linkage to form a 1,4-disubstituted 1,2,3-triazole linkage. Iodine azide was prepared in situ by cooling 0.020 g of sodium azide in 10 mL of acetonitrile (ACN) at 0 °C; 0.013 g of iodine monochloride was then added to the sodium azide solution to form a 10 mM iodine azide solution, and stirred at 0 °C for 15 min before warming to room temperature. Freshly grown carbon nanofiber substrates were immersed in the solution for 3 h at room temperature with gentle stirring of the fluid. The substrates were rinsed with alternating portions of methanol and chloroform before the ethynylferrocene attachment.

The azido-modified VACNF surfaces were linked to ethynylferrocene by immersing them in a solution of 40 μM ethynylferrocene with 0.8 mM Cu(II)(tris-(benzyltriazolylmethyl)amine)SO_4 (TBTA) and 32 mM sodium ascorbate in a 3:1 (v:v) dimethylsulfoxide:H_2O mixture. Samples were rinsed in alternating portions of methanol and chloroform and stored in methanol until further analysis.

The surface bonding of the azide and the subsequent "click" chemistry to link ferrocene to the nanofibers were

(23) Devaraj, N. K.; Decreau, R. A.; Ebina, W.; Collman, J. P.; Chidsey, C. E. D. *J. Phys. Chem. B* **2006**, *110*, 15955.
(24) Merkulov, V. I.; Hensley, D. K.; Melechko, A. V.; Guillorn, M. A.; Lowndes, D. H.; Simpson, M. L. *J. Phys. Chem. B* **2002**, *106*, 10570.
(25) Meyyappan, M.; Delzeit, L.; Cassell, A.; Hash, D. *Plasma Sources Sci. Tech.* **2003**, *12*, 205.
(26) Rice, R. J.; McCreery, R. L. *Anal. Chem.* **1989**, *61*, 1637.
(27) Pinson, J.; Podvorica, F. *Chem. Soc. Rev.* **2005**, *34*, 429.
(28) Brooksby, P. A.; Downard, A. J. *Langmuir* **2004**, *20*, 5038.
(29) Klein, K. L.; Melechko, A. V.; McKnight, T. E.; Retterer, S. T.; Rack, P. D.; Fowlkes, J. D.; Joy, D. C.; Simpson, M. L. *J. Appl. Phys.* **2008**, 103.
(30) Fletcher, B. L.; McKnight, T. E.; Melechko, A. V.; Simpson, M. L.; Doktycz, M. J. *Nanotechnology* **2006**, *17*, 2032.
(31) McKnight, T. E.; Melechko, A. V.; Hensley, D. K.; Mann, D. G. J.; Griffin, G. D.; Simpson, M. L. *Nano Lett.* **2004**, *4*, 1213.
(32) Li, J.; Vergne, M. J.; Mowles, E. D.; Zhong, W. H.; Hercules, D. M.; Lukehart, C. M. *Carbon* **2005**, *43*, 2883.
(33) Li, L.; Lukehart, C. M. *Chem. Mater.* **2006**, *18*, 94.

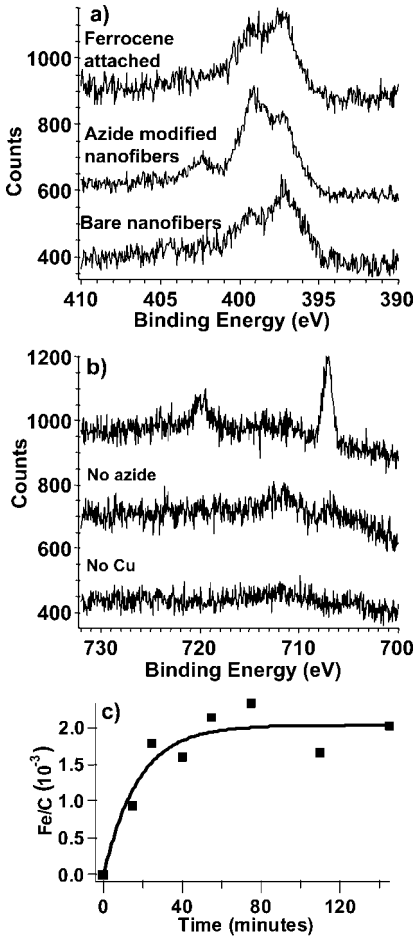

Figure 2. XPS characterization of VACNFs at various stages of functionalization: (a) N(1s) XPS spectrum of as-grown nanofibers, after azide modification, and after grafting of ethynylferrocene; (b) Fe(2p) XPS spectrum of VACNFs after modification with azide and reaction with ethynylferrocene, and control samples in which either the azide treatment or the copper catalyst was intentionally eliminated; (c) kinetic curve of the ferrocene attachment based on XPS iron peaks.

characterized using X-ray photoelectron spectroscopy (XPS). Density functional calculations were used to assist in the interpretation of these data; the results of the calculations and comparison with the experimental spectra are presented in the Supporting Information. Figure 2a shows nitrogen XPS of the VACNFs after each stage of the functionalization. The bare VACNFs have nitrogen peaks at 397 and 399 eV. These peaks arise from nitrogen-containing species in the bulk nanofibers, arising from the ammonia used as a reducing agent and etchant during nanofiber growth. Prior experimental and theoretical results and our own density functional calculations (see the Supporting Information) indicate that the 397 eV peak arises from N bonded to two adjacent C atoms (and an adjacent carbon vacancy), whereas the higher-energy peak at 399 eV arises from three-coordinate N substituting for C in the lattice.[34,35] After the azide attachment, the peak at 399 eV increases in intensity relative to the 397 eV peak, and a new peak at ~402.3 eV is formed. Peaks at similar energies were observed previously after azide treatment of graphitic surfaces of pyrolyzed photoresist.[20] This prior work and our density functional calculations (see the Supporting Information) both indicate that the azido group gives rise to two closely spaced N(1s) peaks at comparatively low binding energy and a third peak ~3 eV higher in binding energy, in agreement with our results. Although the complex structure in the N(1s) region makes quantitative analysis very difficult, the area of the 402.3 eV N(1s) peak is consistent with $\sim 1 \times 10^{14}$ azide groups/cm^2.

No XPS signal due to iodine or iron could be observed on the azido-terminated samples (see the Supporting Information). The absence of iodine is significant because Hassner[37] proposed that IN_3 adds across the carbon double bonds of organic molecules, followed by the elimination of HI.[20,37] Based on the observed C(1s) signal and the noise level in the I(3d) region (spectrum shown in the Supporting Information) we estimate that the density of iodine atoms must be less than $\sim 8 \times 10^{12}$ atoms/cm^2, much less than the density of iron atoms in the ferrocene groups that link to the surface. Thus, our XPS data are consistent with the elimination of iodine predicted by Hassner.[37]

Figure 2 also shows the N(1s) and Fe(2p) regions after the azido-functionalized VACNFs were exposed to ethynylferrocene. Figure 2a shows that exposure to ethynylferrocene removes the peak at 402 eV and reduces the intensity of the peak at 399 eV. Figure 2b shows XPS data for the Fe region after the azido-modified sample was exposed to ethynylferrocene; also included are two control experiments in which either the azide binding step or the copper catalyst was intentionally eliminated. Although the azido-modified sample exposed to ethynylferrocene with the Cu catalyst shows clear $Fe_{3/2}$ and $Fe_{1/2}$ peaks at 720 and 707 eV, the control samples show no detectable intensity from iron. The energies of the Fe peaks are consistent with previously reported values for ferrocene derivatives,[38,39] whereas the absence of intensity in the control samples confirms that the surface linkage occurs via a Cu(I)-catalyzed azide−alkyne cycloaddition.

To ensure that grafting of the ferrocene was as complete as possible, we characterized the rate at which ethynylferrocene reacts with the azido-terminated surface using XPS. Figure 2c shows the ratio of Fe/C(1s) XPS intensities as a function of time. These data show that the reaction reaches maximum coverage after approximately 1 h, after which there is no further reaction. To quantitatively determine the amount of Fe on the surface, the cylindrical shape of the nanofibers must be taken into account; in the Supporting Information we derive this geometric correction and show that for cylindrical fibers with diameter large compared with the inelastic mean free path, the Fe/C intensity ratio is increased by a factor of $(\pi)/(2)$ compared with that expected for a ferrocene layer on a flat surface. Using the known sensitivity

(34) Shalagina, A. E.; Ismagilov, Z. R.; Podyacheva, O. Y.; Kvon, R. I.; Ushakov, V. A. *Carbon* **2007**, *45*, 1808.
(35) Casanovas, J.; Ricart, J. M.; Rubio, J.; Illas, F.; JimenezMateos, J. M. *J. Am. Chem. Soc.* **1996**, *118*, 8071.
(36) Collman, J. P.; Devaraj, N. K.; Eberspacher, T. P. A.; Chidsey, C. E. D. *Langmuir* **2006**, *22*, 2457.
(37) Hassner, A. *Acc. Chem. Res.* **1971**, *4*, 9.
(38) Woodbridge, C. M.; Pugmire, D. L.; Johnson, R. C.; Boag, N. M.; Langell, M. A. *J. Phys. Chem. B* **2000**, *104*, 3085.
(39) Gassman, P. G.; Macomber, D. W.; Hershberger, J. W. *Organometallics* **1983**, *2*, 1470.

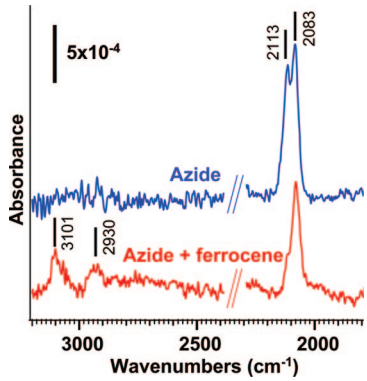

Figure 3. Infrared reflection−absorption spectrum of VACNFs after N_3 attachment, and then after subsequent exposure to ethylnylferrocene.

factor corrections ($S_{Fe} = 2.69$, $S_C = 0.296$)[40] the Fe XPS data yield a coverage of 9×10^{13} ferrocene molecules/cm^2, where this density refers to the number of ferrocene molecules in a given microscopic surface area (as distinct from the projected surface area of the sample).

The N_3 attachment and ferrocene binding were also characterized using infrared spectroscopy, shown in Figure 3. Nanofibers exposed to the azide solution show a closely spaced pair of vibrations at 2083 and 2113 cm^{-1}. These are centered close to the values of 2094[41] and 2105 cm^{-1} [36] reported previously on gold surfaces, confirming the presence of the cumulated double bond (N═N═N) of the azide group on the surface.[42] We note that previous experiments for azides on gold surfaces reported only a single peak,[36,41] whereas we observe two distinct peaks. This suggests the presence of two different N_3 species on the surface. After exposure of the azido-modified sample to ethynylferrocene, Figure 3 shows that there are clear changes in the spectrum. In particular, new peaks appear at 3101 and 2930 cm^{-1}. The peak at 3101 cm^{-1} is nearly identical to the peak at 3104 cm^{-1} attributed to the aromatic C−H stretching in unbound ethynylferrocene and is close to the value of 3113 cm^{-1} observed for ferrocene-terminated monolayers on gold.[43,44] The azide region also shows a substantial reduction in the peak at 2105 cm^{-1}; however, the peak at 2083 cm^{-1} is almost unaffected. This result suggests that the 2105 cm^{-1} peak is very reactive and corresponds to the azido group. The origin of the 2083 cm^{-1} peak remains unknown. Its lack of reactivity and the fact that the XPS data show no appreciable N(1s) signal at high binding energy after reaction with ethynylferrocene suggest that the 2083 cm^{-1} peak likely originates from some other chemical moiety; further studies will be needed to determine its origin.

Electrochemical Properties. Although the XPS and FTIR data clearly establish the presence of covalently bound ferrocene groups on the surface, electrochemical measurements were performed to assess the electrochemical activity of the surface-tethered ferrocene molecules. Figure 4 shows cyclic voltammograms of VACNFs in 1 M $HClO_4$ after covalently linking ferrocene to the surface, along with a control sample consisting of bare nanofibers. The cyclic voltammogram after linking ferrocene shows clear oxidation and reduction peaks at 0.253 and 0.333 V vs Ag/AgCl, indicating that the covalently linked ferrocene molecules are electrochemically active. In contrast, the control sample shows only the trapezoidal-shaped curve characteristic of interfacial capacitance. The vertical separation between the forward and reverse sweeps can be used to estimate the interfacial capacitance, yielding a value of $(2.08 \pm 0.02) \times 10^{-7}$ F. For comparison, identical measurements made on a glassy carbon surface in the same cell yielded $(2.42 \pm 0.17) \times 10^{-8}$ F. Thus, the capacitance measurements suggest that the nanofibers appear to have a microscopic surface area approximately 9 times that of a comparable planar surface with the same projected area. Because the cell has an exposed area of 0.275 cm^2, the capacitance measurements suggest that the nanofibers have a microscopic surface area of 2.47 cm^2.

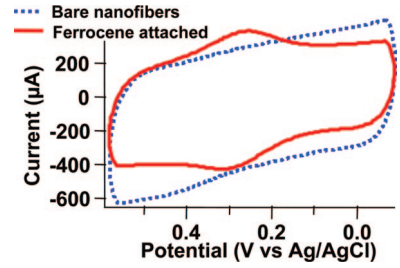

Figure 4. Cyclic voltammograms of the as-grown nanofibers and of nanofibers after modification with azide and then ethynylferrocene. Voltammograms were measured in 1.0 M $HClO_4$, at a scan rate of 1 V/s.

To estimate the number of redox-active groups on the surface, the cyclic voltammetry peaks were integrated, yielding a peak area of $(3.5 \pm 0.3) \times 10^{-5}$ C. Because the ferrocene groups undergo a one-electron redox process, this translates to 2.2×10^{14} redox-active ferrocene groups in the 0.275 cm^2 exposed area, or $(7.9 \pm 0.7) \times 10^{14}$ molecules/cm^2, where the normalization is per unit projected area. Because our capacitance measurements show that the microscopic surface area is ~9 times the projected area, the electrochemical data translate to approximately $(8.8 \pm 0.7) \times 10^{13}$ ferrocene molecules/cm^2 of microscopic surface area. This is similar to the value of $\sim 9 \times 10^{13}$ iron atoms/cm^2 we estimate from our XPS measurements of iron. This value is higher than the 2×10^{13} molecules/cm^2 reported previously from electrochemical measurement of ethynylferrocene bound to pyrolyzed photoresist[20] and is slightly higher than the value of 4.1×10^{13} molecules/cm^2 we estimated for linking ferrocene to VACNFs via a photochemical method.[45]

Electron-Transfer Rates. For strongly adsorbed redox systems with ideal electron-transfer characteristics, the anodic and cathodic peaks are expected to approach the same peak position (thereby yielding zero separation) at very low scan

(40) Moulder J. F.; Stickle W. F.; Sobol P. E.; Bomben K. D. *Handbook of X-ray Photoelectron Spectroscopy*; Perkin-Elmer Corp.: Eden Prarie, MN, 1992.
(41) Fleming, D. A.; Thode, C. J.; Williams, M. E. *Chem. Mater.* **2006**, *18*, 2327.
(42) Socrates, G. *Infrared and Raman Characteristic Group Frequencies*; John Wiley & Sons: New York, 2001.
(43) Viana, A. S.; Abrantes, L. M.; Jin, G.; Floate, S.; Nichols, R. J.; Kalaji, M. *Phys. Chem. Chem. Phys.* **2001**, *3*, 3411.
(44) Viana, A. S.; Jones, A. H.; Abrantes, L. M.; Kalaji, M. *J. Electroanal. Chem.* **2001**, *500*, 290.
(45) Landis E. C.; Hamers. R. J. *J. Phys. Chem. C* **2008**, *112*, 16910.

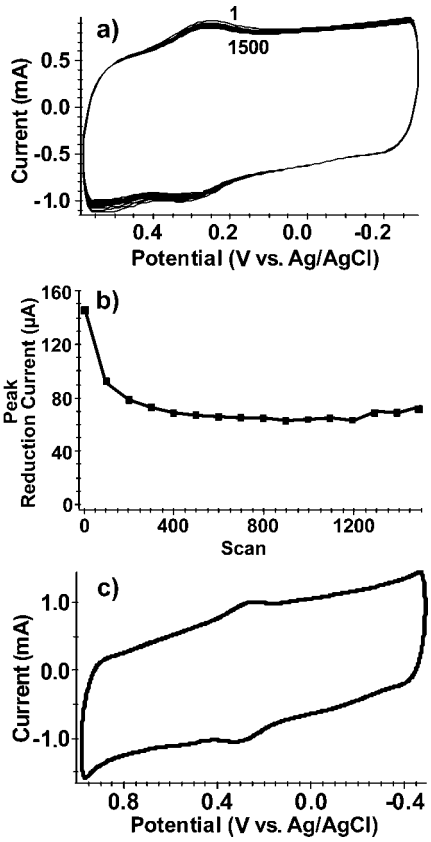

Figure 5. Stability of ferrocene-modified VACNFs: (a) Overlayed voltammograms over 1500 repeated cycles demonstrating the voltage stability of the ferrocene attachment in 1.0 M $HClO_4$, 1 Vs^{1-}, vs Ag/AgCl. The figure shows the first scan and every 100th scan from 100 to 1500. (b) Change in peak reduction current obtained by subtracting the capacitive background from each voltammogram shown in a. (c) Cyclic voltammogram over an extended voltage window, from −0.5 to +1.25 V vs Ag/AgCl.

rates.[46,47] Experimentally, we find that the peak-to-peak splitting for ferrocene attached to VACNF is 80 ± 7 mV at 1 V/s, and decreases to ∼30 mV at 200 mV/s, but does not decrease further. Thus, the electron-transfer characteristics do not reach fully ideal behavior.

The electron transfer rates can be calculated from the cyclic voltammograms using the method of Laviron,[46] who used numerical integration of the rate equations to correlate the standard electron-transfer rate constant k^0 with the separation between cathodic and anodic peaks ΔE_p at different scan rates, v. Using this method to analyze voltammograms obtained at a rate of 1 V/s, we determined that the standard electron transfer rate for ferrocene attached to VACNF surfaces via the "click" chemistry method described here is 1.4 ± 0.2 s^{-1}. Surprisingly, this rate is, within experimental error, identical to the rate of 1.2 ± 0.4 s^{-1} we found using ferrocene molecules linked via longer undecenoic acid molecules.[45]

Electrochemical Stability. A key concern in any surface-tethered electrochemical moiety is the electrochemical stability of the surface-tethered adduct. To test the stability, we conducted multiple cyclic voltammetry experiments. Figure 5a shows each hundredth cyclic voltammetry scan from

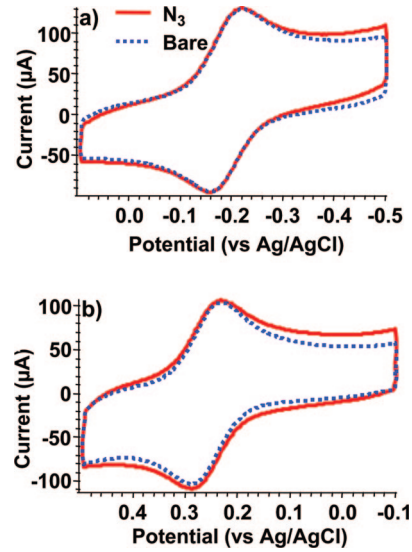

Figure 6. Cyclic voltammetry data of bare and N_3-terminated VACNFs using different redox couples: (a) $Ru(NH_3)_6^{2+/3+}$ redox couple.; (b) $Fe(CN)_6^{3-/4-}$ redox couple.

100−1500. Figure 5b shows the reduction peak current plotted as a function of scan number. Although there is an initial loss of ferrocene during the first 100 scans, subsequent scans show almost no change over as many as 1500 cycles. The ferrocene linkages are also stable at higher voltages as shown in Figure 5c, in which the scan area was increased to −0.5 to +1.0 V vs Ag/AgCl, close to the stability limits of the solvent. Even over this extended potential window, the strong covalent bonding of ferrocene to the underlying nanofibers remains intact.

Electrochemical Determination of Azide Binding Sites. Previous work has shown that the electron-transfer rate constants of many redox couples are sensitive to the surface chemistry of carbon electrodes, which allows us to probe the electron transfer properties of the VACNF electrodes.[26,48,49] Outer-sphere electron transfer systems such as $Ru(NH_3)_6^{2+/3+}$ are insensitive to surface chemistry and their electron transfer rates are determined by the electronic density of states in the substrate material.[48] Previous studies have shown that the electron transfer associated with $Fe(CN)_6^{3-/4-}$ is catalyzed by edge-plane graphite; consequently, electron transfer rates using this redox couple are determined by the ratio of edge plane graphite to basal plane graphite.[26] By performing experiments with both redox couples, the total surface area and the ratio of edge plane graphite to basal plane graphite can be studied.[48,49]

Figure 6a shows cyclic voltammograms of the bare and N_3 terminated VACNF surfaces using the $Ru(NH_3)_6^{2+/3+}$ redox couple. The voltammograms show oxidation and reduction peaks with almost identical peak potentials, with peak-to-peak splittings of 60 ± 3 mV for the bare surface and 61 ± 2 mV for the azido-terminated surface. The nearly identical peak splittings demonstrate that the density of states at the electrode surface has not been altered by the functionalization. However, when the $Fe(CN)_6^{3-/4-}$ redox couple

(46) Laviron, E. *J. Electroanal. Chem.* **1979**, *101*, 19.
(47) Murray, R. W. *Electronal. Chem.* **1984**, *13*, 191.
(48) Chen, P. H.; Fryling, M. A.; McCreery, R. L. *Anal. Chem.* **1995**, *67*, 3115.
(49) Chen, P. H.; McCreery, R. L. *Anal. Chem.* **1996**, *68*, 3958.

was used (Figure 6b), the azido functionalization increases the peak-to-peak splitting from 53 ± 3 mV on the bare VACNF surface to 60 ± 4 mV on the azido-terminated sample. While this increase is only slightly larger than the experimental error associated with multiple measurements, additional comparisons of nearly identical samples suggest that the difference, while small, is real. The slightly slower electron transfer on the azido-terminated surface demonstrates that the azido functionalization reduces the amount of accessible edge-plane graphite. The electrochemical data therefore indicate while the nanofibers expose both edge-plane and basal-plane sites, the azido groups likely bind preferentially at the edge-plane sites. This interpretation is consistent with previous work of Devadoss, et al., who reported that azide functionalization and subsequent ethynylferrocene attachment achieved high densities of attached ferrocene on edge-plane graphite while the reaction with basal-plane graphite did not show significant functionalization.[20]

The width of the cyclic voltammetry peaks can be used to gauge the homogeneity of the monolayer. A layer of independently acting, highly reversible redox centers in identical chemical configurations is expected to yield a full-width at half-maximum (fwhm) of 90.6 mV.[47,50,51] Our measurements show that using "click" chemistry to attach ferrocene molecules yields a significantly wider peak with a fwhm of 147 ± 15 mV. Whereas increased widths can result from interactions among ferrocene molecules, the average distance between molecules is similar to that of prior work on gold surfaces that exhibit nearly ideal behavior.[17] We believe the increased width beyond the ideal value most likely arises from slight inhomogeneities in the chemical environment of the molecules. While nanofibers expose edge-plane sites along their sidewalls, the atomic structure of exposed graphene can vary in a manner similar to the "zig-zag", "armchair", and various chiral terminations of graphene ribbons.[52] The different local surface terminations will likely affect the spatial position and energy of the attached ferrocene molecules.

Discussion

Our results demonstrate that the use of "click" chemistry can be an effective way of linking ferrocene and other redox-active molecules to the surfaces of carbon nanofibers. It is notable that the molecular-level structure of the VACNFs plays a critical role in these results, since our results using $Ru(NH_{36})^{2+/3+}$ and $Fe(CN_6)^{3-/4-}$ redox couples (Figure 6) suggest that the azide coupling occurs preferentially at the edge-plane sites exposed along the nanofiber sidewalls. Transmission electron microscopy measurements of our nanofibers (not shown) confirm the stacked-cup structure, with graphene sheets intersecting the nanofiber surfaces at an angle of intersection of approximately 8°; consequently, the VACNF surfaces consist of rings of exposed edge plane graphite, separated along the axis by approximately 2 nm of basal plane graphite.[53] If ferrocene groups were bonded ~6 Å apart at the exposed edge plane sites and these were separated by 2 nm, this would yield an average density of $\sim 8 \times 10^{13}$ molecules/cm^2, in good agreement with our electrochemical and XPS measurements which show that there are $\sim 9 \times 10^{13}$ ferrocene molecules/cm^2 on the nanofiber sidewalls. Thus, the overall picture of the nanofibers is similar to that depicted in Figure 7, in which ferrocene groups are selectively tethered via the edge-plane sites.

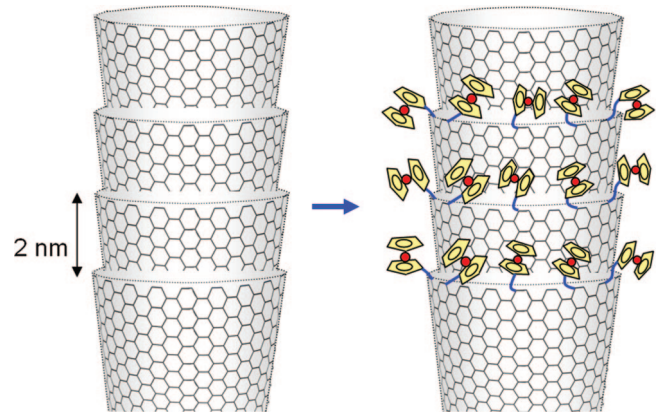

Figure 7. Schematic illustration showing ferrocene groups linked at exposed graphene edge-plane sites. For simplicity, the triazole linkage is not explicitly shown.

One surprising aspect of our work is that the electron transfer rates we measure here using the triazole linkage are only slightly higher than those we found by tethering ferrocene groups to nanofibers via longer alkyl chains. This result is quite different from previous measurements using dense, close-packed layers on gold surfaces, where a strong dependence on length is typically found.[54−58] The most likely explanation for our results is that although molecular layers on surfaces such as gold can form very dense, close-packed layers that block electron transfer,[54,55,59,60] monolayers covalently bound to the nanofibers have a much higher degree of conformational flexibility, as depicted in Figure 7. This flexibility has two consequences.[61−63] First, it means that the ferrocene groups can, on average, be closer to the nanofibers than would otherwise be the case. Second, the ~2 nm separation between edge plane sites is sufficient for intercalation of water between the ferrocene groups. Because the barrier to electron tunneling scales inversely with the

(50) Bard A. J.; Faulkner L. R., *Electrochemical Methods*; John Wiley & Sons: New York, 1980.
(51) Laviron, E. *J. Electroanal. Chem.* **1974**, *52*, 395.
(52) Dutta, S.; Lakshmi, S.; Pati, S. K. *Phys. Rev. B* **2008**, *77*, 073412.
(53) Tse, K. Y.; Zhang, L.; Baker, S. E.; Nichols, B. M.; West, R.; Hamers, R. J. *Chem. Mater.* **2007**, *19*, 5734.
(54) Finklea, H. O.; Hanshew, D. D. *J. Am. Chem. Soc.* **1992**, *114*, 3173.
(55) Finklea, H. O. *Electroanal. Chem.* **1996**, *19*, 109.
(56) Finklea, H. O. *J. Electroanal. Chem.* **2001**, *495*, 79.
(57) Finklea, H. O.; Haddox, R. M. *Phys. Chem. Chem. Phys.* **2001**, *3*, 3431.
(58) Chidsey, C. E. D.; Bertozzi, C. R.; Putvinski, T. M.; Mujsce, A. M. *J. Am. Chem. Soc.* **1990**, *112*, 4301.
(59) Smalley, J. F.; Finklea, H. O.; Chidsey, C. E. D.; Linford, M. R.; Creager, S. E.; Ferraris, J. P.; Chalfant, K.; Zawodzinsk, T.; Feldberg, S. W.; Newton, M. D. *J. Am. Chem. Soc.* **2003**, *125*, 2004.
(60) Weber, K.; Creager, S. E. *Anal. Chem.* **1994**, *66*, 3164.
(61) Napper, A. M.; Liu, H. Y.; Waldeck, D. H. *J. Phys. Chem. B* **2001**, *105*, 7699.
(62) Slowinski, K.; Slowinska, K. U.; Majda, M. *J. Phys. Chem. B* **1999**, *103*, 8544.
(63) Sharp, M.; Petersson, M.; Edstrom, K. *J. Electroanal. Chem.* **1980**, *109*, 271.

dielectric constant of the barrier materials,[63] for a relatively sparse molecular layer in water, the electron-transfer process likely occurs via tunneling through the water rather than through the hydrocarbon chain.

One additional factor controlling the electron-transfer rate is the comparatively low density of states of graphitic materials. The density of states at the basal plane of highly oriented pyrolitic graphite (HOPG) is ~50 times smaller than that of gold, making the exposed basal planes of conventional carbon nanotubes essentially inert electrochemically.[64] In contrast, the presence of exposed edge planes along the sidewalls of the "stacked-cup" VACNFs, combined with their high surface area and the excellent stability of carbon make covalently functionalized VACNFs an attractive support for electrochemical and electrocatalysis studies.

Conclusion

Molecular monolayers can provide a versatile pathway toward formation of complex materials. Our results demonstrate that the Copper-catalyzed azide alkyne cycloaddition (CuAAC) is a facile way to link the unique electrochemical properties of redox-active centers such as ferrocene with the high surface area and chemical stability provided by nanostructured carbon. Our work takes advantage of the fact that unlike conventional single- or multiwall carbon nanotubes, VACNFs expose large amounts of edge-plane graphite along their sidewalls. It is these edge-plane sites that provide the attachment points for the azido groups that after reaction with the alkyne ethynylferrocene serve as covalent linkages between ferrocene and the nanofibers. The ability of the bound ferrocene groups to withstand more than 1500 redox cycles suggests that this type of functionalization may have beneficial use in areas such as electrocatalysis by enabling redox-active or catalytically active molecules to be grafted to nanofibers. Our results demonstrate that "click" chemistry is an excellent way to combine the high surface area, chemical stability, and excellent electrical properties of VACNFs with the unique and rich electrochemical properties of organometallic complexes.

Acknowledgment. This work is supported in part by the National Science Foundation grants DMR0706559 and CHE-0613010. E.C.L. was supported in part by a fellowship from Merck Inc. The authors acknowledge stimulating discussions with Shane Mangold and Professors John Berry and Shannon Stahl.

Supporting Information Available: Iodine XPS spectrum after grafting of ethynylferrocene, comparison of experimental N(1s) spectrum with calculated orbital energies from density functional calculations, complete summary of energies and optimized geometries for azide and methyl triazole linkages at graphene edges, derivation of the geometric correction factor for surface composition of cylindrical carbon nanofibers (PDF). This material is available free of charge via the Internet at http://pubs.acs.org.

CM802869B

(64) Royea, W. J.; Hamann, T. W.; Brunschwig, B. S.; Lewis, N. S. *J. Phys. Chem. B* **2006**, *110*, 19433.